Journal of Atmospheric and Solar-Terrestrial Physics 177 (2018) 247–256

Contents lists available at ScienceDirect

Journal of Atmospheric and Solar-Terrestrial Physics

journal homepage: www.elsevier.com/locate/jastp

Relativistic electron precipitation bands in the outside radiation environment of the International space station

Tsvetan P. Dachev

Space Research and Technology Institute, Bulgarian Academy of Sciences, Acad. G. Bonchev Str. Block 1, 1113 Sofia, Bulgaria

ARTICLE INFO

Keywords:
Space radiation dosimetry
Outer radiation belt
ISS
Relativistic electrons

ABSTRACT

The Radiation risk radiometer-dosimeter (R3DR2) performed active dosimetry measurements outside the International space station (ISS) during the ESA EXPOSE-R2 missions from October 24, 2014 until January 11, 2016. The 10 s resolution flux and dose rate data were used to find, identify and classify the relativistic electron precipitation bands (PB) (Blake et al., 1996) in the outside radiation environment of the ISS. The PB were identified as rapid (10–40-s) dose rate enhancement from the normal (20–200 μGy h^{-1}) outer radiation belt (ORB) level and similar fast return to the same low level. Only PB that have in the time profile dose rates larger than 10,000 μGy h^{-1}, identical to flux larger than 4000 cm^{-2} s^{-1}, for 10 or more seconds were selected. Sixteen PB were studied. The largest selected PB, delivered in the R3DR2 detector, which was behind 0.3 g cm^{-2} shielding, a dose of 464 μGy for 70 s. The later was larger than the ORB daily average dose rates for 366 days out of 442 days measurements during the analyzed period. The daily average doses inside of the ISS were measured, using the DOSTEL instrument, at an average level of 194 μGy d^{-1} (Reitz et al., 2005). This indicates that only for 70 s, the cosmonaut/astronaut, being on extra vehicular activity (EVA), where they are shielded only by their space suits, will accumulate the equivalent of about 2.5-days dose inside of the ISS. Only 1 PB was identified during the ESA EXPOSE-E mission on ISS in the period February 17, 2008–September 3, 2009, while in the more active geomagnetically EXPOSE-R mission in 2010, 6 PB were registered. Although the obtained PB doses do not pose extreme risks for cosmonauts/astronauts health, being on EVA, they have to be considered as a possible extremely high dose rate source, which requires additional comprehensive investigations.

1. Introduction

This paper analyses the space radiation conditions, created by the ORB relativistic electrons, on the ESA EXPOSE-R2 platform, mounted outside the ISS Russian "Zvezda" module. Dachev et al. (2017a), have already published preliminary information for the observed cosmic radiation time profile during the EXPOSE-R2 mission.

The main idea of the paper is to find, identify and classify the relativistic electron precipitation bands (Blake et al., 1996) in the outside radiation environment of the ISS in the period October 24, 2014–January 11, 2016. Short overview of the PB observations outside ISS during the EXPOSE-E (2008–2009) and EXPOSE-R (2009–2010) missions is presented at the end of the paper, too.

1.1. ORB characteristics at the ISS altitude

The Van Allen radiation belts are two regions, encircling the Earth, in which energetic charged particles are trapped inside the Earth's magnetic field. Their properties vary according to solar activity and they represent a hazard to satellites and humans in space (Horne et al., 2005). The ORB is located in the altitudinal range from 3.4 to 10 Earth radii above the equator. The ORB population is electrons with energies less than 10 MeV.

In 2001, we have observed, for the first time, relativistic electrons and/or bremsstrahlung in the US laboratory module of the ISS in the data of the mobile dosimetry unit no. 2 (MDU#2). The latter was a part of the Liulin-E094 instrument (Dachev et al., 2002; Reitz et al., 2005). Because of the relatively small fluxes and dose rates, the effect was not fully understood. Later, the relativistic electrons were steadily observed outside the Foton-M2/M3 spacecraft in the periods May 31–June 16, 2005 and September 14–29, 2007, as well as outside the European Columbus module of the ISS in 2008 (Dachev et al., 2009, 2012a; 2012b). The analysis of the absorbed ORB daily doses, measured outside ISS by the R3DE/R/R2 instruments (Dachev et al., 2013, 2015b, 2017a, 2017b) showed that during the quiet geomagnetic conditions they are at very low levels of a few to a few tens of μGy d^{-1} and do not pose any risk for the astronauts at the time of EVA. It is worth underlining that during EVA

E-mail address: tdachev@bas.bg.

https://doi.org/10.1016/j.jastp.2017.11.008
Received 30 April 2017; Received in revised form 30 September 2017; Accepted 15 November 2017
Available online 21 November 2017

astronauts are shielded only by their space suits, which have shielding characteristics similar to our instruments, i.e. of 0.3 g cm^{-2} (Benton et al., 2006; Cucinotta et al., 2003). The highest ORB daily dose of 2962 μGy d^{-1} was observed with the R3DR2 instrument on 20th of March 2015 at the recovery phase of the geomagnetic storm from March 17. The enhanced, during recovery phase of magnetic storms, ORB daily doses of 2000–3000 μGy d^{-1} are much higher than the other daily sources of galactic cosmic rates (GCR) (80–90 μGy d^{-1}) and inner belt protons (400–500 μGy d^{-1}).

The additional dose rate, measured with DOSTEL instrument outside the ISS due to the enhanced particle flux (EPF) *(this is the term, which was used for the ORB relativistic electrons flux by* Labrenz et al. (2015)*)*, from 24 September to 8 October2004 was calculated to be ~130 μGy d^{-1}. The daily average ORB dose rate, measured with the R3DR2 instrument was more than twice larger (278 μGy d^{-1}), for the period October 24, 2014–January 11, 2016. These values can be explained with the larger geomagnetic activity in the period.

The variations, connected with the geomagnetic activity, represented with the (Disturbance Storm Time) Dst index (http://wdc.kugi.kyoto-u.ac.jp/index.html) or solar wind variations, are with the longest time scale of days. During the quiet time, the doses delivered by the relativistic electron flux in the ORB are at very low levels - up too few tens of μGy d^{-1}. Relativistic electron flux typically decreases, by two or three orders of magnitude, during the main phase of geomagnetic storms and recovers to or increases beyond the pre-storm level during the recovery phase, within several days (Zheng et al., 2006).

Following Blake et al. (1996), the precipitation bands are typically a few degrees in latitude. These bands are often seen in conjugate locations and on consecutive orbits (Blake et al., 1996), suggesting that their tens of seconds duration (as measured by low Earth orbit (LEO) satellites) is due to their spatial rather than temporal, characteristics. Blum et al. (2013) have shown that the precipitation bands can last up to hours and to contribute significantly to the loss of electrons from the ORB. The rapid electron precipitation is often observed at low altitude on a variety of timescales, ranging from short bursts of less than 1 s (microbursts) to a longer duration precipitation, extending a few degrees in latitude.

Blum et al. (2015) investigated the PB that were observed by SAMPEX/HILT instrument (Baker et al., 1993) during 42 high-speed stream-driven storms in 2003–2005 with an average Dst_{min} of ~35 nT. They found that the PB could occur in all epochs of the storm, with a larger occurrence rate in the recovery phase at L value of 4–5. The magnitude of the PB was also increased in the recovery phase, while the L value of the maximum position slightly decrease below L = 5. Blum et al. (2015) mentioned that the PB may be induced by the electromagnetic ion cyclotron (EMIC) waves, which are observed in the inner magnetosphere, primarily in the afternoon sector.

As R3DR2 exposition time is 10 s, microbursts (Blum et al., 2015) are not observable. Yet, the PB structures were registered. The aim of the paper is to study their occurrences and magnitude during the EXPOSE-R2 mission on the ISS. The observed total doses for the PB are analyzed and characterized. The author firmly believes that the obtained for the first time on ISS PB dose rates can be further used for the radiation risk assessment of the astronauts being on EVA.

2. Material and methods

Fig. 1 presents an external view of the R3DR2 instrument, as mounted on the EXPOSE-R2 facility. The R3DR2 instrument is a low mass (0.19 kg), small dimension (76 × 76 × 36 mm) automatic device that measures the solar electromagnetic radiation in four channels and the ionizing radiation in 256 channels. The three solar UV (ultraviolet) and one visible radiation photodiodes are seen in Fig. 1 as small circles on the surface in the central part of the R3DR2 instrument. Their data are not used in this paper. The ionizing radiation detector is located behind the aluminum wall of the instrument and is therefore not visible.

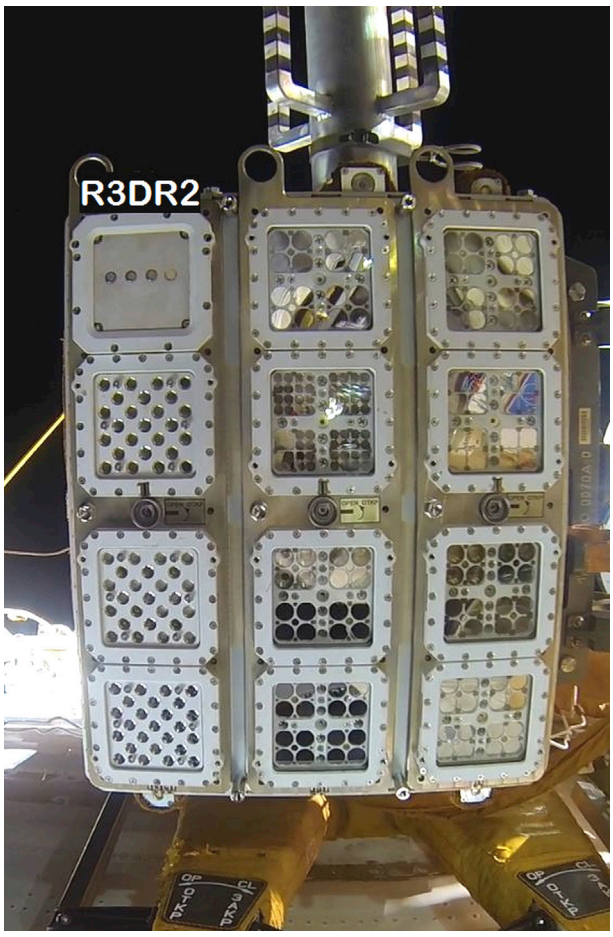

Fig. 1. External view of the R3DR2 instrument as mounted on the EXPOSE-R2 facility. (Picture taken by the Russian cosmonauts G. Pedalka and M. Kornienko on August 15th, 2015 during an EVA to examine the EXPOSE-R2 facility outside the Russian "Zvezda" module.) (Picture credit ESA/RKA).

The R3DR2 instrument is a Liulin type (Dachev et al., 2002, 2015a) deposited energy spectrometer (DES) containing: one semiconductor detector (Hamamatsu (S2744-08) PIN diode 2 cm^2 area, 0.3 mm thick), one charge-sensitive preamplifier, 2 microcontrollers and serial interface of RS425 toward the EXPOSE-R2 facility. Pulse analysis technique is used to obtain of the deposited energy spectrum, which further is used for the calculation of the absorbed dose and the flux in the silicon detector. The two microcontrollers, through specially developed firmware, manage the unit.

The instrument is a successor of the MDUs, developed and used in the Dosimetric Mapping-E094 experiment (Reitz et al., 2005) on the US Laboratory module of the ISS as a part of the Human Research Facility in May–August, 2001 (Dachev et al., 2002). The main purpose of this experiment was to investigate the dose rate distribution inside the ISS. The obtained data were used for the statistical validation of the high-charge and energy (HZE) transport computer (HZETRN) code (Wilson et al., 2007; Nealy et al., 2007; Slaba et al., 2011) and for the validation of the New Trapped Environment AE9/AP9/SPM model at Low Earth Orbit (Badavi, 2014).

The R3D/E/R radiation environment spectrometer-dosimeters on the ESA EXPOSE-E/R platforms were collaboratively developed by Bulgarian and German teams (Häder and Dachev, 2003; Häder et al., 2009). The current R3DR2 spectrometer-dosimeter onboard the ISS is the same instrument that flew in the EXPOSE-R facility from 2009 to 2010. The extension R2 is given to distinguish the data from the two different EXPOSE missions - EXPOSE-R (1) and EXPOSE-R2.

The main measurement unit in the R3DR2 instrument is the amplitude of the pulse after the preamplifier, generated by particles or quanta, hitting the detector (Dachev et al., 2002). The amplitude of the pulse is proportional by a factor of 240 mV MeV^{-1} to the energy loss in the detector and respectively to the dose. By 12 bit analogue to digital converter (ADC) these amplitudes are digitized and organized in a 256-channel deposited energy spectrum. The dose in the silicon detector D_{Si} [Gy] by definition in System international (SI) is one Joule deposited in 1 kg of matter. The absorbed dose is calculated by dividing the summarized energy depositions in the spectrum in Joules to the mass of the detector in kilograms:

$$D_{Si} = K \sum_{i=1}^{255} ik_i A_i MD^{-1} \quad (1)$$

where MD is the mass of the detector in kg, k_i is the number of pulses in channel "i", A_i is the amplitude in volts of the pulses in channel "i", ik_iA_i is the deposited energy (energy loss) in Joules in channel "i". K is a coefficient. All 255 deposited dose values, depending on the deposited energy for one exposure time of 10-s, form the deposited energy spectrum. The energy channel number 256 accumulates all pulses with amplitudes higher than the maximal level of the spectrometer of 20.83 MeV.

DES was calibrated on protons in the Louvain la-Neuve cyclotron facility (Dachev et al., 2002) and on protons and heavy ions at the HIMAC facility in Japan (Uchihori et al., 2002, 2003). In both cases, good agreement was found between the measured and the GEANT code predicted spectra. The post-flight calibrations with Liulin-E094 MDUs were performed on HIMAC heavy ion accelerator during the 1st ICCHIBAN run (Uchihori et al., 2003) in Chiba, Japan, in February 2002 with 400 MeV/u Carbon ions. The spectra, obtained with all the MDUs, showed a sharp maximum in the deposited energy close to 6.1 MeV. This is in good agreement with the theoretical predictions and with the measurements on the same source with DOSTEL-1 instrument (Burmeister et al., 2003).

The calibrations revealed that except for charged energetic particles, the DES has high effectiveness towards gamma rays, which allowed monitoring the natural background radiation (Spurny and Dachev, 2002). Detectors' neutron effectiveness depends on their energy, being minimal for the neutrons with energy 0.5 MeV and has a maximum of few percent for the neutrons with energy 50 MeV in CERN field (Spurny and Dachev, 2003; Silari et al., 2009). According to the "neutron induced nuclear counter effect", introduced for the Hamamatsu PIN diodes of type S2744-08 by Zhang et al. (2011), neutrons could be observed in all channels of the spectrum with at least one order of magnitude larger probability in the first 14 channels. The method, converting D_{Si} to ambient dose equivalent $H^*(10)$ for measurements onboard of an aircraft, was described in (Spurny and Dachev, 2002). Later (Ploc et al., 2011) improved this method.

The semiconductor detector of the R3DR2 instrument was mounted approximately 7 mm below the 0.8 mm thick aluminum cover plate. Furthermore, there was shielding from 0.07 mm copper and 0.2 mm plastic, which provided 0.3 g cm^{-2} of total shielding. The calculated required kinetic energy of particles, arriving perpendicular to the detector, was 0.835 MeV for the electrons and 19.5 MeV for the protons (Berger et al., 2017). This means that only electrons and protons with energies exceeding the values listed above can cross the R3DR2 shielding materials and reach the detector surface.

The R3DR2 instrument was fixed inside EXPOSE-R2 facility (see Fig. 1), which was orientated toward the +Z axes of the ISS, independently from the ISS major attitudes, toward the local zenith. The R3DR2 PIN diode of 2 cm^2 area have an angle of view of about 180° orientated toward the local zenith, during all of the time of the observations. Due to the much thicker shielding of the R3DR2 PIN diode from the side and nadir direction, we believe that in high latitudes we collect mainly ORB precipitating relativistic electrons.

3. Results

3.1. Data selection procedure

The following four primary radiation sources were expected and recognized in the data obtained with the R3DR2 instrument: (i) globally distributed primary GCR particles and their secondary products; (ii) protons in the SAA region of the IRB; (iii) relativistic electrons and/or bremsstrahlung in the high latitudes of the ISS orbit where the ORB is situated; and (iv) solar energetic particles (SEP) in the high latitudes of the ISS orbit. Together with the real SEP particles, a low flux of what were likely to be mostly secondary particles (SP) (protons, neutrons and heavier than H^+ ions) some of them associated with detector interactions were observed in the data.

Recently the data selection procedure described by Dachev et al. (2012b) was upgraded and published by Dachev et al. (2017b). The procedure is based on the experimental formulas for the dose to flux ratio for protons in the range 1–1000 MeV and for electrons in the range 1–10 MeV as published in the book of Haffner (1971). Dachev (2009) demonstrates that according to Haffner's formulas the data can be simply split into two parts by using the dose to flux ratio (D/F). When the measured by the R3DR2 instrument D/F is less than 1.12 nGy cm^2 particle^{-1}, the expected predominant type of radiation in a 10 s interval is ORB electrons. When the D/F is greater than 1.12 nGy cm^2 particle^{-1}, the expected type of radiation is IRB or SEP protons. The GCR source is divided between the two ranges. The new procedure allows the separation of electrons and protons into the internal radiation belt and the electrons and the SEP protons in the outer radiation belt.

3,810,240 10-s measurements were performed in the period October 24, 2014–January 11, 2016. 168,209 of them were identified as generated by predominantly ORB relativistic electrons with energy above 0.835 MeV.

Except the relativistic electrons in the high latitude, a small number of GCR particles exists in the R3DR2 spectra. The minimal number of ORB measurements per day – just 36 10-s measurements, were observed on 11 November 2014. The maximal number of daily ORB measurements, i.e. 1199 observations, were recorded on March 22, 2015, in the recovery phase of the magnetic storm from March 17, 2015. The minimal observed flux/dose rate was 1.1 cm^{-2} s^{-1} and 2.59 μGy h^{-1} respectively, while the maximal observed was 11,813 cm^{-2} s^{-1} and 28,840 μGy h^{-1} respectively.

The obtained daily average ORB absorbed dose rate in the period 24 October 2014–11 January 2015 was 278 μGy d^{-1} with a minimal value of 2.16 μGy d^{-1} on 21 January 2015 and maximal value of 2962 μGy d^{-1} on 20 March 2015. The total delivered ORB dose, in this period, was 123 mGy, which was smaller than the total IRB dose of 251 mGy and larger than GCR total delivered dose of 32 mGy.

3.2. Overview of ORB in the period October 24, 2014–January 11, 2016

Fig. 2 presents information for the variations of the ORB relativistic electrons fluxes and the average daily dose rates, observed between October 24, 2014 and January 11, 2016. There are 5 variables in the figure:

(1) The sum of all channels' counts is presented with red vertical lines against leftmost vertical axes;
(2) The 3 dimensional L value versus time plot presents the maximal observed in the bin flux rate in cm^{-2} s^{-1} against the color bar in the left-upper part of the figure;
(3) The daily averaged dose rates (μGy d^{-1}) are presented by heavy black line against the upper-right vertical axes;
(4) The Dst index variations (http://wdc.kugi.kyoto-u.ac.jp/index.html) in nT are depicted as sky blue line against the lower-right vertical axes;

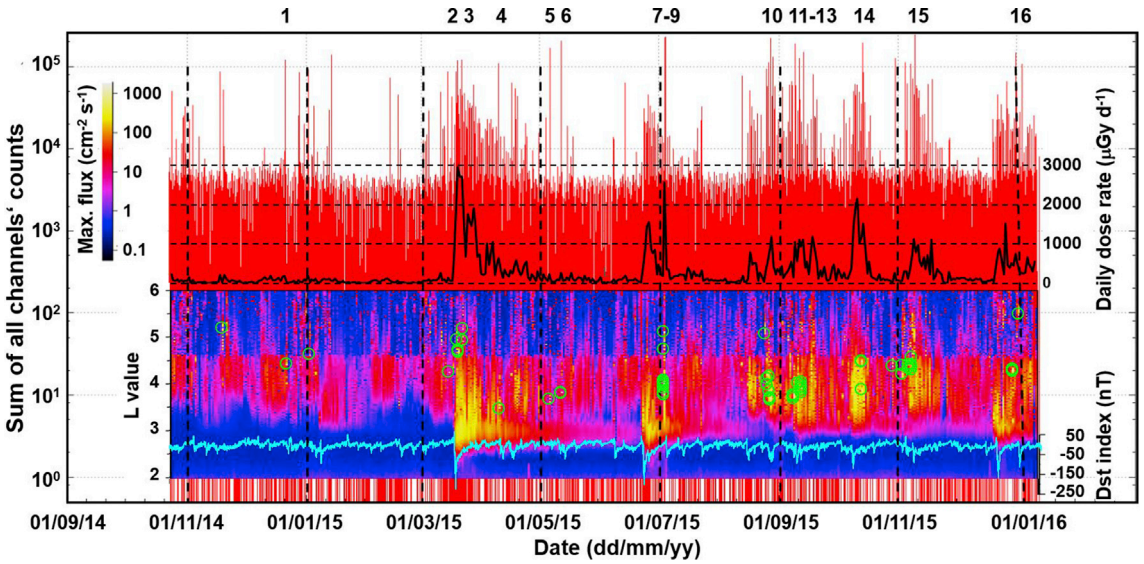

Fig. 2. Variations of the measured with R3DR2 instrument: sum of all channels' counts (red vertical lines); maximal flux (L value versus time plot); daily average dose rate (heavy black line), Dst between 24 October 2014 and 11 January 2016 (Light blue line); positions of the 61 measurements with dose rate higher than 10,000 μGy h^{-1} (light green circles). (For interpretation of the references to colour in this figure legend, the reader is referred to the web version of this article.)

(5) The positions in the L value versus time plot of the observed 61 measurements with a dose rate higher than 10,000 μGy h^{-1} are presented with light green line circles.

The sum of all channels' counts, which is linearly connected with the flux and respectively with the dose rate, is presented with red vertical lines in the background of the figure. The scale is at the leftmost side of Fig. 2 and extends up to more than 200,000 counts per 10 s (equal to a flux of 10,000 cm^{-2} s^{-1}). (Dr. W. Schulte and his colleagues first created these graphics during the EXPOSE-R2 mission support. The author is thankful to Dr. W. Schulte and his colleagues from OHB System AG, München, Germany because the existence of the large single lines in these graphics initiated the interest in the rapid flux enhancements, some of which are identified as PB in this paper.) The smallest sum values of about maximum 70 counts were seen in the magnetic equatorial region, where only primary GCR particles and their secondaries were registered. These bars are not seen in the figure because they are behind the three dimensional plot.

The IRB source red lines extend between 18 and about 7000 counts. The maximal IRB source lines are well seen in the range 3000–7000 counts. The slow variations of the maximal IRB bars level with a minimum in March 2015 and maximum in November 2015 have simple explanation with the variations in the ISS altitude (Dachev et al., 2017b).

Largest red lines up to more than 200,000 counts in Fig. 2 presents the ORB relativistic electrons flux variations. Their existence, density and amplitude are proportional to the daily average ORB relativistic electrons dose rate, seen in the middle of Fig. 2 with heavy black line, which anti-correlates with the Dst variations, presented with light blue line in the bottom of the figure. Single lines, with amplitudes larger than 100,000 counts (5000 cm^{-2} s^{-1}), are associated with possible PB and are object of the study in section 3.3 of the paper.

The 3 dimensional (3D) L value versus time plot in lower part of Fig. 2 presents the variations of the maximal observed, in the bin, relativistic electron flux data (in cm^{-2} s^{-1}) against the color bar in the left-upper part of the figure. The bins with size of 0.02 L value units are organized in a 442 daily vertical bars. They extend between L equal to two and six against the horizontal date axes. The ISS maximal flux bins cover the whole L values range from 2 to 6 in Southern hemisphere, while in the Northern hemisphere the flux data bins are extended only up to L = 4.7, because the Earth magnetic field hemisphere asymmetries. This explain the borderline seen in Fig. 2 at L = 4.7 and the smaller population of the bins in the L range between 4.7 and 6.

The close correlation in Fig. 2 between the ORB count rate, the maximal observed relativistic electron flux and the daily average dose rate is explained with formula (1), which predicts the linear dependence between these parameters and the number of counts in the bins. This phenomenon is well illustrated in many of our previous publications (for example Fig. 3 (Dachev et al. (2016)). The average linear coefficient, that is obtained between 169,609 measurements of all selected as ORB dose rates and fluxes, is equal to 2.4541. From the other hand, 354,249,520 electrons with specific energy of 0.348 nGy per count deposited the total ORB dose of 123 mGy. This value according to Haffner's formula gives an average energy of the electrons of 7.5 MeV, which is larger than expected, because except the electrons a small amount of GCR particles existed in the low energy channels of the spectra. The results is an increase of the specific dose value and the average electrons energy, respectively (Haffner, 1971).

Two periods are clearly seen in Fig. 2 data. In the relatively "quiet" period between October 24, 2014 and the middle of March 2015, the ORB daily dose rate (black curve in Fig. 2) was relatively small and varied in the interval between 2.16 and 260 μGy d^{-1}. In this period, the equatorward boundary of the ORB vary in the interval of L values between 3 and 4. The ORB relativistic electrons equatorward boundary never penetrate at L values below 2.5. The amount and the density of the fast flux enhancements, seen with red vertical lines and light green line circles is also smaller than in the second more disturbed period.

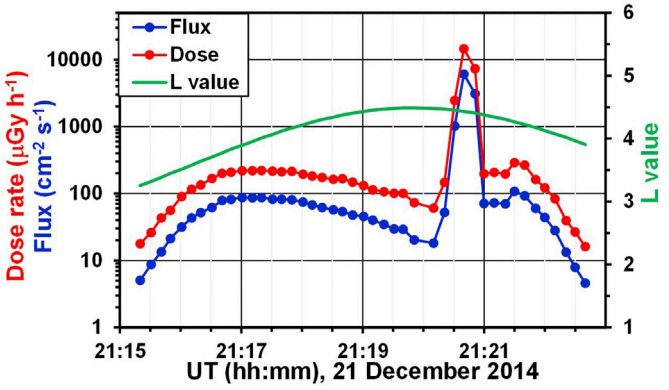

Fig. 3. Single PB on 21 Dec. 2014. 40 μGy were delivered in 10-s.

Four of the totally six daily averaged dose rates occurrences of less than 6 μGy d^{-1} were observed in the quiet period on November 11, 2014, January 21, and on February 22 and 24, 2015. All of these low daily doses, including the one from November 26, 2015, were observed at days with relatively quiet magnetic conditions, when the ORB at the ISS altitudes was practically empty of relativistic electrons. The minimum on 22 June 2015 down to 3.1 μGy d^{-1} occurred in the main phase of the magnetic storm (Zheng et al., 2006).

During the "disturbed" period, between 17 March 2015 and the end of the observations, strong variations in the ORB maximal flux and daily average dose rates were observed, which anti-correlate well with the Dst index variations in the lover part of Fig. 2 (sky blue line). The highest maxima was recorded on 20 March 2015 when the daily average dose rate was 2962 μGy d^{-1} and the averaged for the day flux was 361 cm^{-2} s^{-1}. Higher than 1500 μGy d^{-1} daily average dose rates were observed during another 14 days in the period 19 March - 26 December 2015. Nine of 14 maxima were observed between March 19 and 29, in the recovery phase of the strongest, in the investigated period, magnetic storm on 17 March 2015. After the magnetic storms on June 23 and 25, only one day, 26 June, was with an average dose rate of 1556 μGy d^{-1}. The other 5 days with daily average dose rates higher than 1500 μGy d^{-1} were: 4 of July, 10, 11 and 14 of October and 26 of December 2015. The average dose rate from these 14 days is about 2000 μGy d^{-1}, which is more than 7 times higher than the daily average over the whole EXPOSE-R2 measurement period of 278 μGy d^{-1}.

The penetration of relativistic electrons down to L values of about 2.4 and the strong temporary enhancements of the maximal flux, seen in the 3D plot of Fig. 2, usually takes place in the main phase of the magnetic storm, when the negative value of Dst is large (Zheng et al., 2006). Later, during the recovery phase of the magnetic storm, the ORB equatorial boundary moved from about L = 2.4 back to L = 3.0. These features were repeatedly registered during the storms in March, June and December 2015. Most of the time the ORB was with single maximum distribution in the L profile but after the storms in March and June, periods with two maxima were registered. The best example of two maxima L distribution profile, seen in Fig. 2, is the period between May 20 and June 20, 2015. The two maxima L distribution profiles were detected mainly in the southern hemisphere. The two maxima in the L profile are additionally studied in Fig. 7.

Similarly to Claudepierre et al. (2017) and Turner et al. (2017), we start to record penetration of the relativistic electrons below L = 2.5 on 18 March 2015. In the period March 18–28 the lower boundary of L = 2 was reached. Then the relativistic electrons at low L disappeared on March 28th. The storm on June 25th generated again fluxes of the ORB relativistic electrons at L values below 2.5 and they are clearly seen in Fig. 2. The ORB enhancement on 4th July 2015 emphasized them again

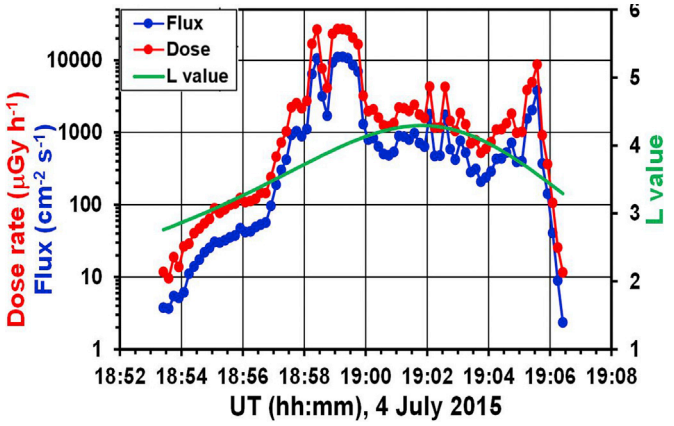

Fig. 4. The left side maximum registered on 4 July 2015, which contains 7 points above 10,000 μGy h^{-1} was identified as PB. 464 μGy were delivered in 70-s.

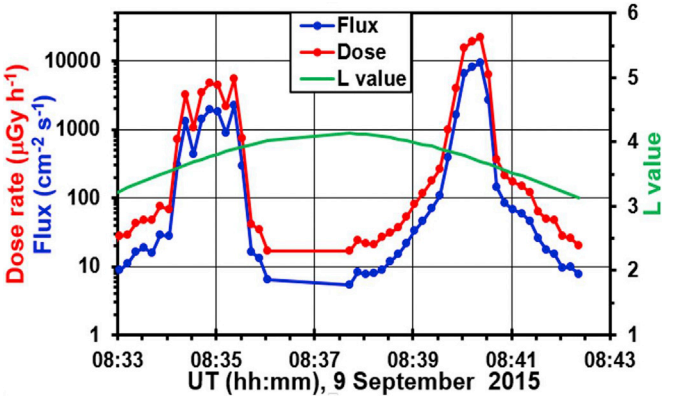

Fig. 5. The right side maximum, which contains 3 points above 10,000 μGy h^{-1} was identified as PB on 9 September 2015. 157 μGy were delivered in 30-s.

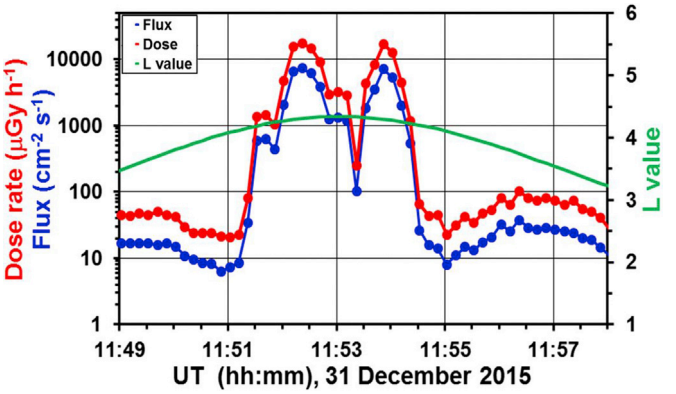

Fig. 6. The two large PB on 31 December 2015. Totally 214 μGy were deliver in 50-s.

but at this case the minimal L values reached was L = 1.6 (For more details please see next part of the paper). Almost all disturbances in the Dst from July 11th, 2015 until January 1st, 2016 generated a new portion of relativistic electrons in the range of L values between 1.6 and 2. They existed for 1–2 days and disappeared until the next Dst disturbance.

The 3D L value versus time plot in Fig. 2 are compared with the analogical plots in the same periods as observed by MagEIS instrument at NASA's Van Allen Probes mission (Claudepierre et al., 2017). It is found that the R3DR2 3D variations of the daily averaged maximal fluxes are very similar to the corrected for background contamination variations of the 1.06 and 1.58 MeV daily average electron fluxes, presented in Fig. 3 by Claudepierre et al. (2017). The similarity of our 3D plot with the MagEIS instrument 0.9 MeV 3D plot, presented in Fig. 1 by Turner et al. (2017), confirm the selection procedure of the ORB data. The time profiles of the relativistic bands below L = 2.5 also look very similarly.

3.3. *Identification and characterization of the precipitation bands*

Sporadic, short time-scale relativistic electron high fluxes, presented with larger than 100,000 counts vertical red lines and with white bins in the 3D graphic are observed in Fig. 2. 61 light green line circles that were selected under the requirement the dose rate to be higher than 10,000 μGy h^{-1} additionally emphasized the positions of the bins with possible PB. The high fluxes bins in the 3D graphic were seen preferably in disturbed periods. This well-seen tendency appears in the L range between 3.5 and 5.5.

The higher than 100,000 counts lines in Fig. 2, which simultaneously show higher than 4000 cm^{-2} s^{-1} flux, were specially selected and numerated from 1 to 16. Events that have duration from 10 to 70-s and extended in few degrees in latitude, were classified as potential

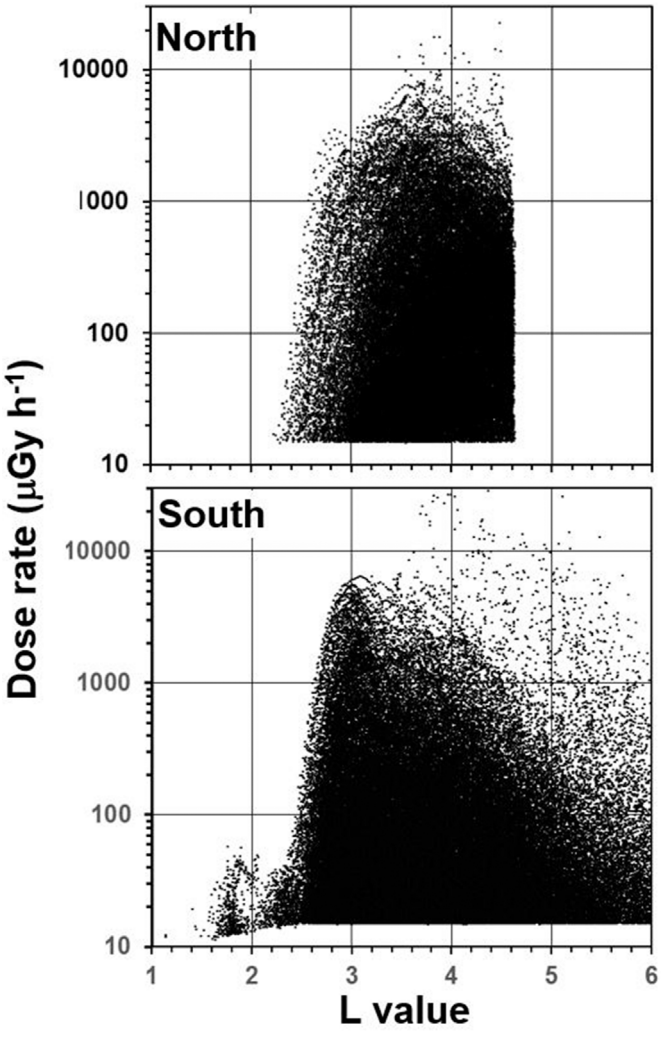

Fig. 7. A comparison of the L-value dose rate distributions of the Northern (upper panel) and the Sothern (lower panel) magnetic hemispheres.

precipitation bands (PB) (Blake et al. (1996)).

PB was identified as rapid enhancement from the usual (100–2000 μGy h^{-1}) ORB level and similar fast return to the same low level. Only rapid (in 10–20 s) enhancement in the time profile above 10,000 μGy h^{-1} and above ~ 4000 cm^{-2} s^{-1} for 10 or more seconds were selected.

Table 1 presents the result of the investigation of the potential PB numbered from 1 to 16 seen in the upper part of Fig. 2. On 4 July 2015 three PB were found. From the studied 16 cases only 1 does not reveal clear characteristics of PB.

Finally, the 16 PB were studied in Table 1. Most of the PB did not last more than 30 s, but one was 50 s and another was 70 s. The average L value of the PB was L = 4.24. Most of the PB were found in negative Dst values in the different phase of small and moderate magnetic storms and substorms. Detailed look in Fig. 2 confirms this result.

The analysis of the accumulated doses, shown in the last column of Table 1, reveals the following:

- The July 4th 10-s PB at 12:47 UT delivered a dose of 73 μGy, which was larger than the average daily doses for 151 days out of 443 days during the analyzed period;

Table 1
The results of the investigation of the potential PB numbered from 1 to 14 in Fig. 2.

No	Date (dd/mm/yyyy)/Time (hh:mm)/Comment	Result	Dst value (nT)	Maximal dose rate (μGy h^{-1})/Flux (cm^{-2} s^{-1})	Delivered dose (μGy)/No of rel. electr.
1	21/12/2014 21:20 **See** Fig. 3	10-s PB	−22	14,547/6075	40 in 10-s. 121,480
2	20/03/2015 06:31	30-s PB	−58	13,623 5888	101 in 30-s 315,540
3	22/03/2015 07:53	20-s PB	−43	14,003 6035	70 in 20-s 220,500
4	10/042015 01:21	10-s PB	−33	12,722 5413	35 in 10-s 108,260
5	06/05/2015 11:36	10-s PB	−18	19,481 8326	54 in 10-s 166,520
6	12/05/2015	Not clearly seen PB at low L value.			
7	04/	10-s PB	15	26,262	**73 in 10-s**
8	072015	10-s PB	32	10,297 10,884	205,940
9	12:47 14:24 18:59 **See** Fig. 4	70 s PB	−7	4569 27,020 11,164	30 in 10 s 91,380 **464 in 70-s** 1,365,760
10	27/08/2015 18:21	10-s PB	−77	25,588 10,532	71 in 10-s 210,640
11	09/09/2015 08:40 **See** Fig. 5	30-s PB	−92	21,997 9314	157 in 30-s 478,840
12	11/09/2015 08:23	10-s PB	−13	14,769 5684	41 in 10-s 113,680
13	13/09/2015 13:45	50-s PB	−33	17,998 7412	214 in 50-s 633,400
14	14/10/2015 01:12	20-s PB	−41	22,712 9408	101 in 20-s 305,800
15	09/11/2015 15:12	30-s PB	−52	28,840 11,813	117 in 20-s 348,920
16	31/12/2015 11:52 31/12/2015 11:55 **See** Fig. 6	30-s PB 20-s PB	−5 −5	17,482 7343 16,821 7186	132 in 30-s 399,120 82 in 20-s 249,660

- The July 4^{Th} 70-s PB at 18:59 UT delivered a dose of 464 μGy h^{-1}, which was larger than the average daily doses for 366 days out of 443 days during the analyzed period.

The daily average doses reported by Reitz et al. (2005) inside of the ISS were measured using the DOSTEL instrument at an average level of 194 μGy day^{-1} (Reitz et al., 2005, p. 379). This indicates that due to the 70 s PB on July 4th, the cosmonaut/astronaut outside the ISS will accumulate the equivalent of about 2.5-day dose inside of the ISS (just for several seconds).

Figs. 3–6 present graphics with 4 examples of PB that were prepared in similar way:

- The UT of the day of the observations is plotted on the horizontal axes;

- The dose rate (red points and curve) in μGy h^{-1} and flux (blue points and curve) in cm^{-2} s^{-1} are plotted against the left vertical axes;
- The L value with heavy green line is plotted against the right vertical axes.

Fig. 3 shows a PB with 1 measurement of dose rate above 10,000 μGy h^{-1}, which is seen with rapid rise from the normal ORB level of 80 μGy h^{-1} and similar fast return to the level of 300 μGy h^{-1}. The PB occurred at about 21:20 UT on December 21st, 2014 in the pre-storm period of moderate magnetic storm with the main phase of −51 nT at 05:00 UT on December 22, 2014. Relatively small dose of 40 μGy was delivered. The PB in Fig. 3 is very similar to the published PB by Blake et al. (1996) (see Fig. 3 therein).

Fig. 4 presents data for the longest and largest, in Table 1, PB on July 4th, 2015 around 19:00 UT. This PB occurred during the main phase of moderate geomagnetic storm. The PB was identified with the rapid enhancement from the ORB level of 120 μGy h^{-1} and similar fast return to the level of 2000 μGy h^{-1}. The right side maximum in Fig. 4 was not identified as PB because the dose rate was smaller than 10,000 μGy h^{-1}. The structure of data in Fig. 4 is similar to the two PB structures in Figs. 5 and 6. The delivered dose of 464 μGy by this PB is the largest observed during EXPOSE-R2 mission.

Fig. 5 presents data for the PB observed in the main phase of moderate magnetic storm with Dst index of −94 nT at 09:00 on 9 of September 2015. Only the right, larger enhancement, was selected as PB in the study, because the dose rate in the left hand maximum was not higher than 10,000 μGy h^{-1}. The Fig. 5 data can be interpret also as two PB in conjugate locations. The first smaller PB is centered at 145° East longitude, while the second at 174° East longitude. Similar is the situation with the two PB presented in Fig. 6, registered on 31 of December 2015 in the pre-storm phase of the magnetic storm with Dst = −117 nT at 00:00 h on January 1st, 2016. In Figs. 5 and 6, the PB appear at some smaller L value, disappear when ISS moves to higher L values and appear again, when the station returns to the same smaller L value. The above reveals that the PB were extended like an oval around the magnetic pole and is a strong proof that the PB are spatial structures.

The statistical analysis of the 61 measurements (light green line circles in Fig. 2), with dose rate higher than 10,000 μGy h^{-1} (flux higher than 4000 cm^{-2} s^{-1}), gives the following results:

1) The PB occurred mainly in the pre-storm and in the main phase of the magnetic storm. Only 3 PB were observed in the less disturbed period until the middle of March 2015. The PB flux and the dose rate values were higher for more disturbed period;
2) The PB occurred more frequently in Southern hemisphere (44 occurrences out of 61). To clear the hemispheric differences was prepared Fig. 7, which presents the L value profiles of the ORB dose rate in the Northern and Sothern magnetic hemispheres. 169,609 measurements of ORB was divided by the requirements the dipole latitude (Dlat) to be less or more than zero. Upper panel of Fig. 7 presents L value distribution in the Northern magnetic hemisphere, while the lower panel in Sothern.

The first large difference is generated by the Earth magnetic field hemisphere asymmetries. As shown in Fig. 7 the ISS orbit with inclination of 51.6° in Northern hemisphere reached L values not larger than 4.7, while in the Sothern hemisphere the ISS reached L values of 6 (really 6.2 but here this small part is not presented). This difference allows the ISS to accumulate 102,403 measurements in the Southern and only 67,206 in the Northern magnetic hemisphere. The average flux and dose rate in the Northern hemisphere (133 cm^{-2} s^{-1} and 336 μGy h^{-1}) were larger than in the Southern (85 cm^{-2} s^{-1} and 212 μGy h^{-1}) one.

The Northern hemisphere L value distribution is clearly with one maximum at L = 3.6, while the Sothern shows two maxima: a larger at L = 3 and a smaller at L = 4. Closer view in Fig. 2 reveals that two maxima was observed in some of the days of June, July and August 2015. The two maxima of the L-value distributions were classified by Mann et al. (2016) as the "third" Van Allen radiation belt.

The points with dose rate larger than 10,000 μGy h^{-1} are well seen in both hemispheres. These points in the Northern hemisphere were often above the main maxima of the ORB L value distribution, while in the Southern they appear out of the region of the main maximum at L = 3.

The dose rates of the events, with penetration of the relativistic electrons below L = 2.5, are well seen in the Southern hemisphere distribution in Fig. 7. Small dose rate values and respectively the flux of these events confirm the conclusions made by Claudepierre et al. (2017) that the relativistic electrons in slot region and inner zone do have small fluxes and sporadic character;

3) PB covered the following geographic coordinates: in the Northern hemisphere from 120° to 105° West longitude and from 48° to 51.6° North latitude. In the Southern hemisphere from 50° to 175° East longitude and from −45° to 51.6° South latitude. The measured average dose rate values were larger in the southern hemisphere (North = 14,127 μGy h^{-1}; South = 16,366 μGy h^{-1})
4) PB covered L coordinates from 3.5 to 5.5 with well seen tendency of maximum occurrences and maximum amplitude at L = 4.0;
5) PB were observed more frequently in the dusk local magnetic times and the values were larger for the same period, too. Fig. 8 illustrates the different behavior of the ORB flux profiles at different magnetic local times (MLT) in the both hemispheres. The flux data in dependence from UT on 4 July 2015 are plotted with heavy black line. The "ex" form markers in flux line present the points of consequence measurements with 10 s resolution. The 12 maxima seen in Fig. 8 show the ORB flux variation in 12 sub sequential ISS crossings of L > 2.4 regions, i.e. 6 crossings of the Northern and 6 crossings of the Southern hemisphere. First crossings in the left side of Fig. 8 is in the Northern hemisphere, next is in the Southern hemisphere and so on. The green line in Fig. 8 represents the Dst index variations (http://wdc.kugi.kyoto-u.ac.jp/index.html). It Illustrates that the R3DR2 flux data was obtained in the initial and very first hours of the main phase of a moderate geomagnetic storm (Gonzalez et al., 1994).

In Fig. 8 it is seen that the sub sequential flux points in the Northern hemisphere crossings are going smoothly, following the form of L value, presented with red points in Fig. 8. The Southern hemisphere crossings show fast variations in the flux value. When the flux value is over 4000 cm^{-2} s^{-1} (black dashed horizontal line in Fig. 8) this point is classified as ORB "precipitation band". Most drastic is the difference between the Northern hemisphere time profile at about 18:15 UT and the next one in the Southern hemisphere at about 19:00 UT, when the longest and the largest PB (shown in Fig. 4) was observed. Never the less that the L profiles seen in Fig. 8 of both transits seems to be very similar. The main difference in both transits is in the magnetic local time (MLT), which variations are illustrated with blue line in Fig. 8. The Northern hemisphere transit is at average MLT = 11:00, while the Southern hemisphere transit is at MLT = 22:00. Similar are the MLT differences for all the 6 pairs of the Northern/Southern hemispheres transits.

According to the literature analysis made by Blum et al. (2015): "the PB during more active times may be induced by electromagnetic ion cyclotron (EMIC) waves … In the inner magnetosphere, these waves are observed primarily in the afternoon sector, where anisotropic ring current ions overlap cool, dense plasmaspheric plumes."

More precise analysis shows that the 44 points with dose rate higher than 10,000 μGy h^{-1} of 61 in the Southern hemisphere occurred at average MLT = 20:00. The maximum, observed during the EXPOSE-R2 mission, flux (11,813 cm^{-2} s^{-1}) and dose rate (28,840 μGy h^{-1}) values were found at about 22:30 local magnetic time;

6) A PB dependence from the altitude of the ISS was not found, most probably because of the small range of the altitudes of the PB observations.

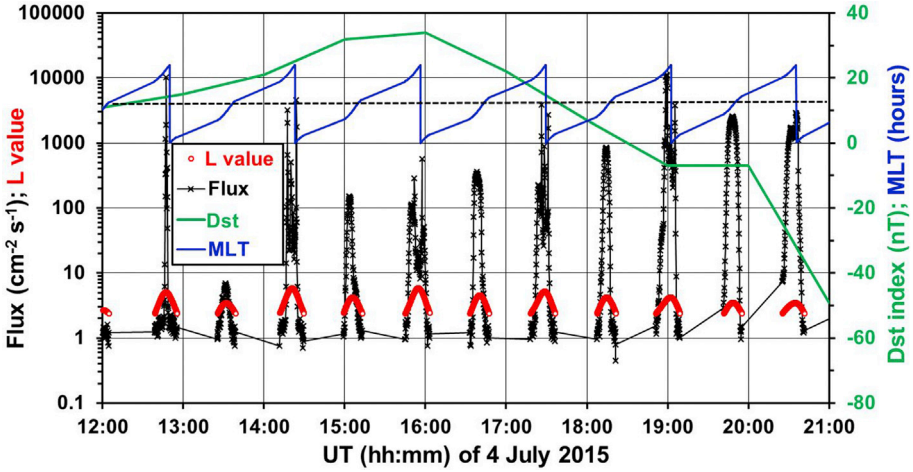

Fig. 8. There are 4 variables in the figure: the heavy black line plots the flux with 10-s resolution in dependence from UT on 4 July 2015; the red points present the L-value variations; the blue line presents the variations of the MLT, while the green line shows the Dst variations. This figure illustrates the different behavior of the ORB flux profiles at different magnetic local times (MLT) in both hemispheres. (For interpretation of the references to colour in this figure legend, the reader is referred to the web version of this article.)

3.4. PB observations during EXPOSE-E and EXPOSE-R (1) missions

R3DE instrument measurements during EXPOSE-E mission took place between February 17, 2008 and September 3, 2009 (Dachev et al., 2012b). This was the quietest mission on the ISS from geomagnetic activity point of view that is why only one PB, with dose rate above 10,000 μGy h^{-1}, was observed on February 28, 2008 at 11:24 UT. The PB time profile was similar to the one presented in Fig. 3, with a single dose rate point above the normal ORB maximum level. The PB occurred in the pre-phase of a small magnetic storm with minimal Dst = −52 nT on 28 of February at 23:00 UT.

R3DR(1) instrument was used during EXPOSE-R (1) mission between March 11, 2009 and August 20, 2010 (Dachev et al., 2012a; 2015b). The period between 1st of March 2009 and 1st of March 2010 was characterized by a low solar and geo-magnetic activity, which was the main reason for the low ORB activity and lack of PB. The R3DR and GOES-11 daily relativistic electrons fluences increased on 6 and 7 of April 2010. Although the magnetic storm on April 6 2010 was moderate (minimal Dst = −72 nT at about noon), the second largest values in history of GOES fluences of electrons with energies >2 MeV were measured (Dachev et al., 2012a). The increase in the GOES-11 fluence of electrons with energies more than 2 MeV was by 4.5 orders of magnitude, whereas the R3DR daily fluences and daily absorbed dose rates increased less than 3.5 orders of magnitude (Dachev et al., 2013).

On the 6th of March 2010 a single point PB was observed at 09:54:50 UT with a maximal dose rate of 10,928 μGy h^{-1}. The next PB at 13:03:34 UT was again a single point one, with an amplitude of 21,132 μGy h^{-1}. This PB is very well seen in Fig. 3 of Dachev et al. (2013) but it was not mentioned as a PB. There was another PB on the 6th of April 2010 at 14:36:11 UT but it happen in descending L values and the equatorward fast decrease of the dose rate was not clearly seen.

On April 7 and 9 2010, another 24 events, with dose rates higher than 10,000 μGy h^{-1}, were registered but they were without fast risings and returns profiles and were interpreted as very large smoot ORB enhancements. The largest daily dose rate for the EXPOSE-R mission was observed on April 7, 2010 and was 2323 μGy d^{-1}. It is smaller than the largest EXPOSE-R2 mission record of 2962 μGy d^{-1} on March 20, 2015.

Three more PB were observed for less than 5 min interval on May 30, 2010 close to 18:09 UT and 24:00 h MLT. They were created in response to a moderate geomagnetic storm with a minimal Dst = −80 nT about noon on 29 of May. The total number of observed PB during the EXPOSE-R mission is six.

4. Discussion and conclusions

The most important achievement of this article is the discovery and the proof of the existence of precipitation bands in the relativistic electrons dose rates outside the ISS during the EXPOSE missions in the period 2008–2016. The PB was identified as rapid enhancement from the usual (100–2000 μGy h^{-1}) ORB dose rate level and similar fast return to the same low level. Only rapid (10–20 s) enhancement in the time profile above 10,000 μGy h^{-1} and above ~ 4000 cm^{-2} s^{-1} with a duration of 10 or more seconds were selected. One PB was identified in the EXPOSE-E data in the quietest, from geomagnetic activity point of view, period in 2008–2009. Six PB were observed in April–May 2010 during EXPOSE-R mission.

During the EXPOSE-R2 mission in the period from 24 October 2014 to 11 January 2016 from the examined 16 cases 15 were proved to be real PB. Total of 61 measurements with dose rates higher than 10,000 μGy h^{-1} were found and analyzed.

The analysis of the absorbed daily doses, obtained by the R3DR2 instrument, show that during the quiet geomagnetic conditions they are at very low levels of a few to few tens of μGy d^{-1}. Thus, they do not pose any serious risk for the astronauts being on EVA. During EVA astronauts' only protection is their space suits. The latter has shielding characteristics similar to the R3DR2 instrument, i.e. of 0.3–0.5 g cm^{-2} (Benton et al., 2006; Cucinotta et al., 2003). In the case of very high daily relativistic electrons enhancements, like on March 20–22 2015, the daily absorbed dose increased up to 2700 μGy d^{-1} or even more, which is much higher than the other daily sources of GCR (80–90 μGy d^{-1}) and inner belt protons of 400–500 μGy d^{-1}.

It was found that the ORB enhancement between 12:46 and 20:39 UT on 4 of July 2015 delivered a total dose of 2.44 mGy by fluence of 7,142,700 particles. The daily average doses, reported by Reitz et al. (2005) inside of the ISS, measured by DOSTEL instrument, were at an average of 194 μGy day^{-1} (Reitz et al., 2005, p. 379). This indicates that during the ORB enhancement for 8 h, the cosmonaut/astronaut outside the ISS will accumulate the equivalent of about 12.5-day dose inside of the ISS. This result can be further used to evaluate the risks for the cosmonauts/astronauts being on EVA.

The PB were classified as hazardous to the health of cosmonauts/astronauts on EVA because:

1) A single point PB delivered for 10 s accumulated dose of 73 μGy. This dose was larger than the daily doses for 151 days (out) of 443 days during the analyzed period;

2) The 70 s dose of 464 μGy on 4 July 2015 at 19:00 UT was larger than the daily doses for 366 days out of 443 days during the analyzed period. The daily average doses reported by Reitz et al. (2005) inside of the ISS were 194 μGy day^{-1} (Reitz et al., 2005, p. 379). This indicates that only for 70-s, the cosmonaut/astronaut outside the ISS will accumulate the equivalent of about 2.5-day dose inside of the ISS.

The PB on the ISS occurred mainly in negative Dst conditions in the Southern hemisphere. The PB coordinates were distributed as an oval around the magnetic poles. The precipitation bands covered L coordinates from 3.5 to 5.5 with well seen tendency of maximum at L = 4. The PB were observed more frequently in the dusk local magnetic times and the values were larger for the same period, too. Blum et al. (2015) mentioned that the PB during more active times may be induced by the electromagnetic ion cyclotron (EMIC) waves, which are observed in the inner magnetosphere, primarily in the afternoon sector. The maximum observed flux (11,813 cm^{-2} s^{-1}) and dose rate (28,840 μGy h^{-1}) values were at about 22:30 local magnetic time.

The main conclusion of the presented data is that the ORB enhancements and the PB events are common on the ISS. Although the obtained doses do not pose extreme risks for the astronauts, being on EVA, they have to be considered as a permanently detected radiation source, which requires additional comprehensive investigations.

Acknowledgements

The author is grateful to the following colleagues: N. Bankov, B. Tomov, P. Dimitrov and Y. Matviichuk from Space Research & Technology Institute at the Bulgarian Academy of Sciences for the cooperation in the development of the R3DR2 spectrometer and for the assistance with data analysis; G. Horneck, D.P. Häder, and G. Reitz for the overall German–Bulgarian cooperation in the Biopan and EXPOSE projects. The author is also grateful to the colleagues from DLR, in Germany and to Dr. W. Schulte and his colleagues from OHB System AG, in München, Germany for the EXPOSE-R2 mission support.

This work was partially supported by Contract No. 4000117692/16/NL/NDe funded by the Government of Bulgaria through an ESA Contract under the Plan for European Cooperating States (PECS).

The R3DR2 data used in this paper are part of the above mentioned contract entitled: “DOSIMETRY: Dosimetry science payloads for ExoMars TGO & surface platform; Unified web-based database with Liulin-type instruments' cosmic radiation data”. This is the reason why the R2DR2 dose rate and flux data and some time-spatial coordinates of the ISS are currently available online at the following URL: http://esa-pro.space.bas.bg/node/23. Later they will be part of the database.

References

Badavi, F.F., 2014. Validation of the new trapped environment AE9/AP9/SPM at low Earth orbit. Adv. Space Res. 54, 917–928. https://doi.org/10.1016/j.asr.2014.05.010.

Baker, D.N., Mason, G.M., Figueroa, O., Colon, G., Watzin, J.G., Aleman, R.M., 1993. An overview of the solar anomalous, and magnetospheric particle explorer (SAMPEX) mission. Geoscie. Remote Sens. IEEE Trans. 31 (3), 531–541.

Benton, E.R., Benton, E.V., Frank, E.V., Moyers, M.F., 2006. Characterization of the radiation shielding properties of US and Russian EVA suits using passive detectors. Radiat. Meas. 41, 1191–1201.

Berger, M.J., Coursey, J.S., Zucker, M.A., Chang, J., 2017. Stopping-power and Range Tables for Electrons, Protons, and Helium Ions. NIST Standard Reference Database 124. Available online at: http://www.nist.gov/pml/data/star/index.cfm.

Blake, J.B., Looper, M.D., Baker, D.N., Nakamura, R., Klecker, B., Hovestadt, D., 1996. New high temporal and spatial resolution measurements by SAMPEX of the precipitation of relativistic electrons. Adv. Space Res. 18 (8), 171–186.

Blum, L.W., Schiller, Q., Li, X., Millan, R., Halford, A., Woodger, L., 2013. New conjunctive CubeSat and balloon measurements to quantify rapid energetic electron precipitation. J. Geophys. Res. Let. 40, 5833–5837. https://doi.org/10.1002/2013GL058546.

Blum, L., Li, X., Denton, M., 2015. Rapid MeV electron precipitation as observed by SAMPEX/HILT during high-speed stream-driven storms. J. Geophys. Res. Space Phys. 120, 3783–3794. https://doi.org/10.1002/2014JA020633.

Burmeister, S., Beaujean, R., Petersen, F., Reitz, G., 2003. Post flight, calibration of DOSTEL with heavy ions during the first and third, ICCHIBAN run at HIMAC, Chiba. In: 8th Workshop on Radiation Monitoring for the International Space Station 3–5 September 2003. LBNL, Berkeley, USA. Available online at: http://wrmiss.org/workshops/eighth/burmeister.pdf.

Claudepierre, S.G., et al., 2017. The hidden dynamics of relativistic electrons (0.7-1.5 MeV) in the inner zone and slot region. J. Geophys. Res. Space Phys. 122. https://doi.org/10.1002/2016JA023719.

Cucinotta, F.A., Shavers, M.R., Saganti, P., Miller, J., 2003. Radiation Protection Studies of International Space Station Extravehicular Activity Space Suits. NASA/TP-2003–212051, December 2003.

Dachev, TsP., 2009. Characterization of near Earth radiation environment by Liulin type instruments. Adv. Space Res. 1441–1449. https://doi.org/10.1016/j.asr.2009.08.007.

Dachev, Ts, Tomov, B., Matviichuk, Yu, Dimitrov, Pl, Lemaire, J., Gregoire, Gh, Cyamukungu, M., Schmitz, H., Fujitaka, K., Uchihori, Y., Kitamura, H., Reitz, G., Beaujean, R., Petrov, V., Shurshakov, V., Benghin, V., Spurny, F., 2002. Calibration results obtained with Liulin-4 type dosimeters. Adv. Space Res. 30, 917–925. https://doi.org/10.1016/S0273-1177(02)00411-8.

Dachev, TsP., Tomov, B.T., Matviichuk, YuN., Dimitrov, P.G., Bankov, N.G., 2009. Relativistic electrons high doses at international space station and Foton M2/M3 satellites. Adv. Space Res. 1433–1440. https://doi.org/10.1016/j.asr.2009.09.023.

Dachev, TsP., Tomov, B.T., Matviichuk, YuN., Dimitrov, PlG., Bankov, N.G., Reitz, G., Horneck, G., Häder, D.-P., Lebert, M., Schuster, M., 2012a. Relativistic electron fluxes and dose rate variations during april-may 2010 geomagnetic disturbances in the R3DR data on ISS. Adv. Space Res. 50, 282–292. https://doi.org/10.1016/j.asr.2012.03.028.

Dachev, Ts, Horneck, G., Häder, D.-P., Lebert, M., Richter, P., Schuster, M., Demets, R., 2012b. Time profile of cosmic radiation exposure during the EXPOSE-E mission: the R3D instrument. J. Astrobiol. 12 (5), 403–411. http://eea.spaceflight.esa.int/attachments/spacestations/ID501800a9c26c2.pdf.

Dachev, TsP., Tomov, B.T., Matviichuk, YuN., Dimitrov, PlG., Bankov, N.G., Reitz, G., Horneck, G., Häder, D.-P., Lebert, M., Schuster, M., 2013. Relativistic electron fluxes and dose rate variations observed on the international space station. J. Atmos. Solar-Terrestrial Phys. 99, 150–156. https://doi.org/10.1016/j.jastp.2012.07.007.

Dachev, T.P., Semkova, J.V., Tomov, B.T., Matviichuk, YuN., Dimitrov, P.G., Koleva, R.T., St Malchev, Bankov, N.G., Shurshakov, V.A., Benghin, V.V., Yarmanova, E.N., Ivanova, O.A., Häder, D.-P., Lebert, M., Schuster, M.T., Reitz, G., Horneck, G., Uchihori, Y., Kitamura, H., Ploc, O., Kubancak, J., Nikolaev, I., 2015a. Overview of the Liulin type instruments for space radiation measurement and their scientific results. Life Sci. Space Res. 4, 92–114. https://doi.org/10.1016/j.lssr.2015.01.005.

Dachev, Ts, Horneck, G., Häder, D.-P., Schuster, M., Lebert, M., 2015b. EXPOSE-R cosmic radiation time profile. J. Astrobiol. 14, 17–25. https://doi.org/10.1017/S1473550414000093.

Dachev, T.P., Tomov, B.T., Matviichuk, Yu N., Dimitrov, Pl G., Bankov, N.G., 2016. High dose rates obtained outside ISS in June 2015 during SEP event. Life Sci. Space Res. 9, 84–92. https://doi.org/10.1016/j.lssr.2016.03.004.

Dachev, T.P., Bankov, N.G., Horneck, G., Häder, D.-P., 2017a. Letter to the Editor. Radiat. Prot. Dosim. 174 (2), 292–295. https://doi.org/10.1093/rpd/ncw123.

Dachev, T.P., Tomov, B.T., Matviichuk, YuN., Dimitrov, Pl G., Bankov, N.G., Horneck, G., Häder, D.-P., 2017b. Overview of the ISS radiation environment observed during EXPOSE-R2 mission in 2014-2016. Space Weather. https://doi.org/10.1002/2016SW001580 accepted for publication on 25 September 2017.

Gonzalez, W.D., Joselyn, J.A., Kamide, Y., Kroehl, H.W., Rostoker, G., Tsurutani, B., Vasyliunas, V.M., 1994. What is a geomagnetic storm?'. J. Geophys. Res. 99, 5771–5792.

Häder, D.-P., Dachev, T.P., 2003. Measurement of solar and cosmic radiation during spaceflight. In: Surveys in Geophysics, vol 24. Kluwer Press, pp. 229–246.

Häder, D.P., Richter, P., Schuster, M., Dachev, Ts, Tomov, B., Georgiev, Pl, Matviichuk, Yu, 2009. R3D-B2-Measurement of ionizing and solar radiation in open space in the BIOPAN 5 facility outside the FOTON M2 satellite. Adv. Space Res. 43 (8), 1200–1211. https://doi.org/10.1016/j.asr.2009.01.021.

Haffner, J.W., 1971. Yadernoe Izluchenie I Zashchita V Kosmose (Nuclear Radiation and Protection in Space), pp 115, Atomizdat, Moscow, (book in Russian), translated from: J.W. Haffner, Radiation and shielding in space. Ac. Press, NY, 1967.

Horne, R.B., Thorne, R.M., Shprits, Y.Y., Meredith, N.P., Glauert, S.A., Smith, A.J., Kanekal, S.G., Baker, D.N., Engebretson, M.J., Posch, J.L., Spasojevic, M., Inan, U.S., Pickett, J.S., Decreau, P.M.E., 2005. Wave acceleration of electrons in the Van Allen radiation belts. Nature, 2005/09/08/online, 437|8 September 2005. https://doi.org/10.1038/nature03939.

Labrenz, J., Burmeister, S., Berger, T., Heber, B., Reitz, G., 2015. Matroshka DOSTEL measurements onboard the international space station (ISS). J. Space Weather Space Clim. 5, A38. https://doi.org/10.1051/swsc/2015039.

Mann, I.R., Ozeke, L.G., Murphy, K.R., Claudepierre, S.G., Turner, D.L., Baker, D.N., Rae, I.J., Kale, A., Milling, D.K., Boyd, A.J., Spence, H.E., 2016. Explaining the dynamics of the ultra-relativistic third Van Allen radiation belt. Nat. Phys. 12 (10), 978–983.

Nealy, J.E., Cucinotta, F.A., Wilson, J.W., Badavi, F.F., Zapp, N., Dachev, T., Tomov, B.T., Semones, E., Walker, S.A., Angelis, G. De, Blattnig, S.R., Atwell, W., 2007. Pre-engineering spaceflight validation of environmental models and the 2005 HZETRN simulation code. Adv. Space Res. 40 (11), 1593–1610. https://doi.org/10.1016/j.asr.2006.12.030.

Ploc, O., Spurny, F., Dachev, TsP., 2011. Use of energy depositing spectrometer for individual monitoring of aircrew. Radiat. Prot. Dosim. 144 (1–4), 611–614. http://rpd.oxfordjournals.org/content/early/2010/12/24/rpd.ncq505.abstract.

Reitz, G., Beaujean, R., Benton, E., Burmeister, S., Dachev, T., Deme, S., Luszik-Bhadra, M., Olko, P., 2005. Space radiation measurements on-board ISS-The DOSMAP experiment. Radiat. Prot. Dosim. 116 (1–4), 374–379.

Silari, M., Agosteo, S., Beck, P., Bedogni, R., Cale, E., Caresana, M., Domingo, C., Donadille, L., Dubourg, N., Esposito, A., Fehrenbacher, G., Fernández, F., Ferrarini, M., Fiechtner, A., Fuchs, A., García, M.J., Golnik, N., Gutermuth, F., Khurana, S., Klages, Th, et al., 2009. Intercomparison of radiation protection devices in a high-energy stray neutron field. Part III: instrument response. Radiat. Meas. 44, 7–8, 673-691.

Slaba, T.C., Blattnig, S.R., Badavi, F.F., Stoffle, N.N., Rutledge, R.D., Lee, K.T., Zapp, E.N., Dachev, T.P., Tomov, B.T., 2011. Statistical validation of HZETRN as a function of vertical cutoff rigidity using ISS measurements. Adv. Space Res. 47, 600–610. https://doi.org/10.1016/j.asr.2010.10.021.

Spurny, F., Dachev, T., 2002. On board aircrew dosimetry with a semiconductor spectrometer. Radiat. Prot. Dosim. 100, 525–528. http://rpd.oxfordjournals.org/cgi/content/abstract/100/1-4/525.

Spurny, F., Dachev, T.s., 2003. Long-term monitoring of the onboard aircraft exposure level with a Si-Diode based spectrometer. Adv. Space Res. 32 (1), 53–58. https://doi.org/10.1016/S0273-1177(03)90370-X.

Turner, D.L., et al., 2017. Investigating the source of near-relativistic and relativistic electrons in Earth's inner radiation belt. J. Geophys. Res. Space Phys. 122, 695–710. https://doi.org/10.1002/2016JA023600.

Uchihori, Y., Kitamura, H., Fujitaka, K., Dachev, TsP., Tomov, B.T., Dimitrov, P.G., Matviichuk, Y., 2002. Analysis of the calibration results obtained with Liulin-4J spectrometer-dosimeter on protons and heavy ions. Radiat. Meas. 35, 127–134. http://www.sciencedirect.com/science/article/pii/S1350448701002864.

Uchihori, Y., Kitamura, H., Fujitaka, K., Yasuda, N., Benton, E., 2003. Comparison of results from the 1st ICCHIBAN experiment and current status of the 3rd ICCHIBAN Experiment. In: 8th Workshop on Radiation Monitoring for the International Space Station 3–5 September, LBNL. Berkeley, USA. Available online at: http://wrmiss.org/workshops/eighth/uchihori.pdf.

Wilson, J.W., Nealy, J.E., Dachev, T., Tomov, B.T., Cucinotta, F.A., Badavi, F.F., Angelis, G. de, Leutke, N., Atwell, W., 2007. Time serial analysis of the induced LEO environment within the ISS 6A. Adv. Space Res. 40 (11), 1562–1570. https://doi.org/10.1016/j.asr.2006.12.030.

Zhang, L., Mao, R., Zhu, R., 2011. Fast neutron induced nuclear counter effect in Hamamatsu silicon PIN diodes and APDs. IEEE Trans. Nucl. Sci. 58 (3), 1249–1256. http://www.hep.caltech.edu/~zhu/papers/11_tns_fast_neutron.pdf.

Zheng, Y., Lui, A.T.Y., Li, X., Fok, M.-C., 2006. Characteristics of 2–6 MeV electrons in the slot region and inner radiation belt. J. Geophys. Res. 111, A10204. https://doi.org/10.1029/2006JA011748.